Astron. Astrophys. 362, 133–137 (2000)

ASTRONOMY AND ASTROPHYSICS

# ISO far-infrared observations of rich galaxy clusters⋆

## III. Abell 2029, Abell 2052, Abell 2142

**L. Hansen[1], H.E. Jørgensen[1], H.U. Nørgaard-Nielsen[2], K. Pedersen[2], P. Goudfrooij[3,⋆⋆], and M.J.D. Linden-Vørnle[1,2]**

[1] Copenhagen University Observatory, Juliane Maries Vej 30, 2100 Copenhagen, Denmark
[2] Danish Space Research Institute, Juliane Maries Vej 30, 2100 Copenhagen, Denmark
[3] Space Telescope Science Institute, 3700 San Martin Drive, Baltimore, MD 21218, USA

Received 28 April 2000 / Accepted 25 August 2000

**Abstract.** A sample of five rich galaxy clusters has been mapped by ISO at $60\,\mu$m, $100\,\mu$m, $135\,\mu$m, and $200\,\mu$m using the PHT-C camera. In previous papers Abell 2670 and Sérsic 159-03 were discussed. Here we present the results for Abell 2029, Abell 2052, and Abell 2142. The conclusion of the survey is that the relatively small fields (≈60 square arc minutes) are structured with filaments or superpositions of point sources. In some cases point sources ($\approx 0.1$ Jy) can be identified with cluster galaxies. An attempt to demonstrate infrared emission from dust in the cooling flows (due to star formation) was inconclusive.

**Key words:** galaxies: clusters: individual: Abell 2029, Abell 2052, Abell 2142 – infrared: galaxies

### 1. Introduction

The central parts of 5 rich galaxy clusters have been mapped by the Infrared Space Observatory (ISO) satellite, using the PHT-C camera (Lemke et al. 1996) at $60\,\mu$m, $100\,\mu$m, $135\,\mu$m, and $200\,\mu$m. In paper I (Hansen et al. 1999) and paper II (Hansen et al. 2000) the results for Abell 2670, respectively Sérsic 159-03 were presented and discussed. In Abell 2670 we identified three far-infrared sources apparently related to star forming galaxies in the cluster. Infrared emission from the dominant cD galaxy was difficult to ascertain in the complicated field and with the limited resolution, but any flux from the cD is fainter than from the three detected sources. In the Sérsic 159-03 field – for which we have two similar observations separated by 4 weeks and covering almost the same field – a source is present at the position of the central cD. The fluxes in the four bands ($\approx 0.05$ Jy) are roughly consistent with a simple model predicting the production of dust grains due to star formation in the cooling flow. Optical data suggest, however, that the cD is undergoing a merger event, and the dust grains could also come from infalling gas clouds evaporating in the hot interstellar/intra-cluster medium. For three other off-center sources we were not able to identify optical counterparts.

We here present the results for the last three clusters for which some useful data are given in Table 1. Redshift and richness class are taken from the NASA/IPAC Extragalactic Database[1]. Data for the cooling flows are from White et al. (1997). The mean electron density, $\bar{n}_e$, within the cooling radius, $R_{cool}$, was obtained from the average radial profile of the electron density (White et al. 1997, Fig. 12) scaled to give the gas mass within 0.5 Mpc for the individual objects (White et al. 1997, Table 4).

**Table 1.** Cluster redshift and richness from the NED and cooling radius, temperature, mass-deposition rate, and mean density in the cooling region for the X-ray cluster gas (White et al. 1997)

| Object | redshift | richness class | $R_{cool}$ | kT keV | $\dot{M}$ $M_\odot\ yr^{-1}$ | $\bar{n}_e$ $cm^{-3}$ |
|---|---|---|---|---|---|---|
| Abell 2029 | 0.0767 | 2 | $1'.1$ | 7.2 | 298 | 0.007 |
| Abell 2052 | 0.0332 | 0 | $1'.5$ | 3.3 | 54 | 0.004 |
| Abell 2142 | 0.0899 | 2 | $0'.5$ | 11.4 | 106 | 0.015 |

### 2. Observations

#### *2.1. The ISO data*

The ISO observations were performed as oversampled maps in the PHT 32 mode as described in paper I. The $60\,\mu$m and $100\,\mu$m bands were obtained with the 9 pixel C100 detector, while the 4 pixel C200 detector was used for the $135\,\mu$m and $200\,\mu$m bands. The size of the mapped areas and the target dedicated times (TDT) are given in Table 2. The data were batch pro-

*Send offprint requests to*: L. Hansen ((leif@astro.ku.dk)

⋆ Based on observations with ISO, an ESA project with instruments founded by ESA member states (especially the PI countries: France, Germany, the Netherlands, and the United Kingdom) and with the participation of ISAS and NASA

⋆⋆ Affiliated to the Astrophysics Division, Space Science Department, European Space Agency

[1] The NASA/IPAC Extragalactic Database (NED) is operated by the Jet Propulsion Laboratory, California Institute of Technology, under contract with the National Aeronautics and Space Administration

**Table 2.** Log of the ISO observations. TDT is the target dedicated time (seconds)

| Object | date | mapped area | | TDT | |
|---|---|---|---|---|---|
| | | C100 | C200 | C100 | C200 |
| Abell 2029 | 26 Aug 1996 | $5\farcm3 \times 11\farcm5$ | $6\farcm1 \times 12\farcm5$ | 2030 | 2081 |
| Abell 2052 | 27 Aug 1996 | $8\farcm4 \times 12\farcm9$ | $9\farcm2 \times 13\farcm9$ | 3683 | 5714 |
| Abell 2142 | 8 Sep 1996 | $3\farcm8 \times 9\farcm9$ | $4\farcm6 \times 10\farcm9$ | 1747 | 1788 |

**Table 3.** Source fluxes (Jy) determined from the Abell 2052 PIA maps by positioning, scaling, and subtracting the PSF. The quoted uncertainties are *not* statistical, but are subjectively evaluated limits

| object | $100\,\mu$m | $135\,\mu$m | $200\,\mu$m |
|---|---|---|---|
| A2052-2 | $0.16 \pm 0.07$ | $0.40 \pm 0.10$ | $0.22 \pm 0.06$ |
| A2052-3 | $0.21 \pm 0.07$ | $0.25 \pm 0.12$ | $0.25 \pm 0.12$ |
| A2052-4 | $0.07 \pm 0.04$ | $0.09 \pm 0.05$ | $0.12 \pm 0.06$ |

cessed by the ISOPHOT Interactive Analysis software[2] (PIA, version V7.1.1e) as described in paper I. Parallel reductions using a more simple least squares reduction procedure (LSQ, see paper I) were also performed for comparison. Our experience from paper I and paper II is that PIA or both PIA and LSQ occasionally produce spurious sources, but if a source is present at several wavelengths and/or in repeated observations we consider it as real.

The resulting PIA maps are presented in Figs. 1, 3, and 5. The pixel sizes are $15'' \times 46''$ for C100 and $30'' \times 92''$ for C200, although the instrumental resolution is only about $50''$ for C100 and $95''$ for C200. It applies to all maps that up is towards west (approximately) with north to the left. The areas covered by the C200 maps are shown in Figs. 2, 4, and 6 which are optical images of the fields extracted from the Digital Sky Survey[3].

## 3. Discussion

### *3.1. Abell 2029*

The intra-cluster gas of Abell 2029 is very regular and smooth suggesting a relaxed cluster (Sarazin et al. 1998), and a substantial cooling flow is present (White et al. 1997, Sarazin et al. 1998). Inspection of the PIA maps (Fig. 1) does not reveal any certain sources. A structure in the C200 maps is seen (particularly at $135\,\mu$m) running upwards from the middle of the lowest row passing the center to the right. Experience from paper II shows that such structures can be real as they reappear in repeated observations. Inspection of Fig. 2 does not reveal any significant correlation between this infrared feature and optical objects.

### *3.2. Abell 2052*

The $135\,\mu$m and $200\,\mu$m brightness maps for Abell 2052 (Fig. 3) show some sources which are likely to be real. Two of these, A2052-2 and A2052-3, are also present at $100\,\mu$m and coincide (see Fig. 3) with galaxies sharing the cluster redshift according to NED. One or more sources are present northeast of A2052-3 at $135\,\mu$m and $200\,\mu$m. A fainter source, A2052-4, has no clear optical counterpart. As in paper I and paper II we estimate the source fluxes by positioning, scaling and subtracting the PSF from the maps. The scale factor is varied and the success in removing the source is evaluated by eye. In that way we estimate the maximum and minimum acceptable flux, and the median and its deviation from the limits are given in Table 3.

The central cD galaxy is not associated with any certain infrared emission. Some enhanced emission, A2052-1, is seen at $135\,\mu$m and $200\,\mu$m about $1'$ northwest of the cD, i.e. just outside the excess X-ray emission found by Rizza et al. (2000), but we are unable to point out any striking candidate for an optical counterpart to A2052-1.

### *3.3. Abell 2142*

Markevitch et al. (2000) recently presented *Chandra* observations which show that the intra-cluster gas of Abell 2142 is strongly nonisothermal, and they interpret the data as the result of a late stage merger between two clusters. A cooling flow of $\dot{\mathrm{M}} = 69^{+70}_{-\ldots}\ \mathrm{M}_\odot\ \mathrm{yr}^{-1}$ may still be present, but is not strongly required by their data. These conclusions are essentially equivalent to the Henry & Briel (1996) results.

The infrared brightness maps presented in Fig. 5 show no convincing features at $60\,\mu$m and $100\,\mu$m. Some broad features seen at $135\,\mu$m and $200\,\mu$m seem real, but no optical counterparts can be pointed out. Two bright X-ray sources — a Seyfert galaxy and a narrow-tail radio galaxy mentioned by Markevitch et al. (2000) — have no infrared counterparts. Nor is there any infrared brightness enhancement associated with the X-ray maximum and temperature minimum shown by their Fig. 3.

### *3.4. Dust in cooling flows*

A major motivation for initiating this investigation of far-infrared emission from rich galaxy clusters was to test the hypothesis, that dust is continuously formed and destroyed in cooling flows. Assuming that most of the cooling gas ends up in low mass stars, dust grains could grow in the cold pre-stellar gas phase. After star formation a certain fraction ($\approx 10\%$) of the cool, dust-enriched gas is recycled to the hot gas phase. Here the grains are heated by hot electrons and – to some extent – by optical photons. They are, however, also hit by ions and eroded

[2] The ISOPHOT data presented in this paper was reduced using PIA, which is a joint development by the ESA Astrophysics Division and the ISOPHOT consortium

[3] Based on photographic data of the National Geographic Society – Palomar Observatory Sky Survey (NGS-POSS) obtained using the Oschin Telescope on Palomar Mountain. The NGS-POSS was funded by a grant from the National Geographic Society to the California Institute of Technology. The plates were processed into the present compressed digital form with their permission. The Digitized Sky Survey was produced at the Space Telescope Science Institute under US Government grant NAG W-2166

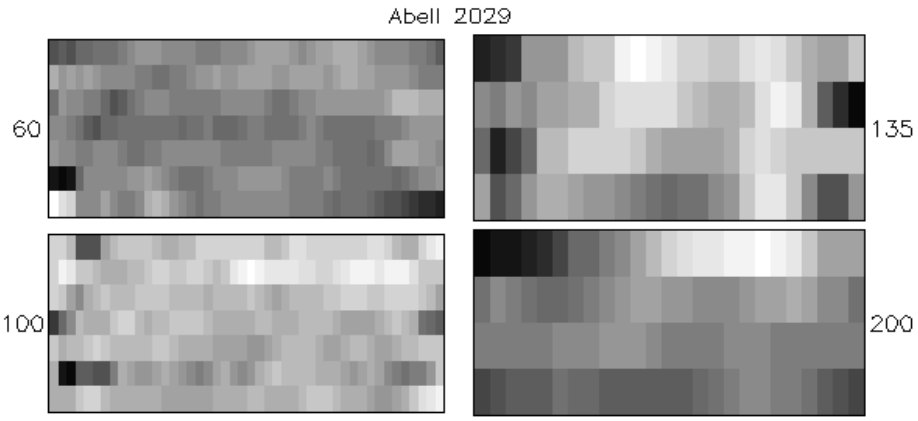


**Fig. 1.** The brightness maps are shown for Abell 2029 for the four pass-bands. Maximum brightness is dark. Value ranges in $\mathrm{MJy\,sr^{-1}}$ are: 12.3–17.7 ($60\,\mu\mathrm{m}$), 8.3–11.6 ($100\,\mu\mathrm{m}$), 9.0–9.8 ($135\,\mu\mathrm{m}$), 5.0–7.6 ($200\,\mu\mathrm{m}$). Left is approximately towards north and up towards west. Compare with the optical image of the field shown in Fig. 2

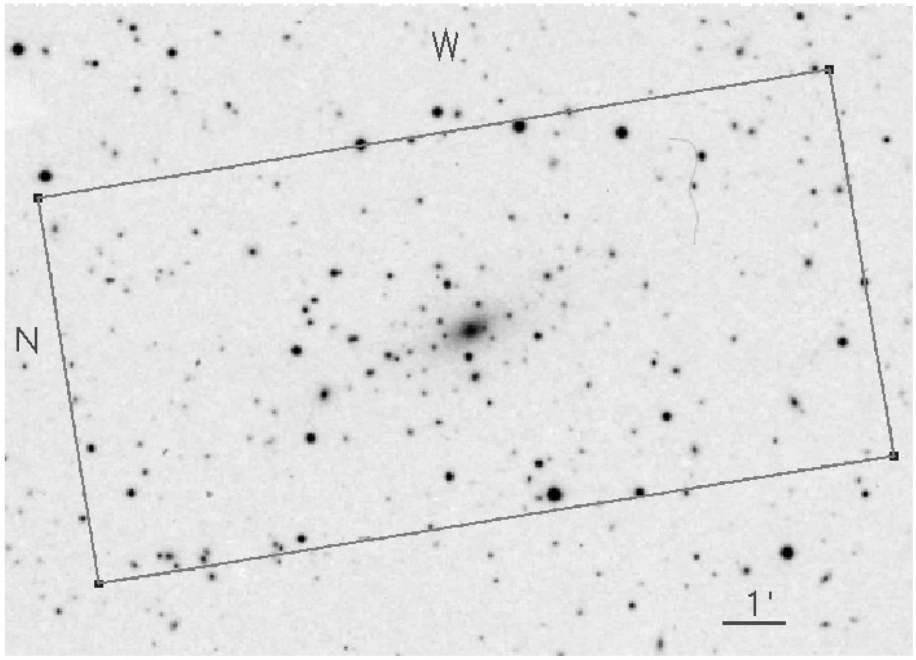


**Fig. 2.** The central field of Abell 2029 showing the boundaries of the C200 map. North is to the left and west is up to ease comparison with Fig. 1

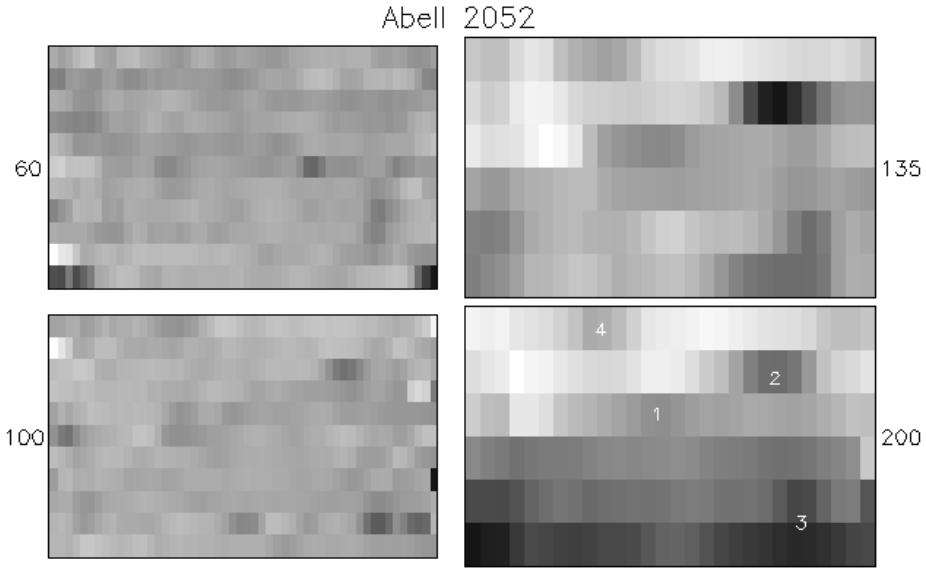


**Fig. 3.** The brightness maps are shown for Abell 2052 for the four pass-bands. Maximum brightness is dark. Value ranges in $\mathrm{MJy\,sr^{-1}}$ are: 10.4–16.4 ($60\,\mu\mathrm{m}$), 6.4–11.5 ($100\,\mu\mathrm{m}$), 8.1–9.6 ($135\,\mu\mathrm{m}$), 4.5–6.1 ($200\,\mu\mathrm{m}$). Left is approximately towards north and up towards west. Compare with the optical image of the field shown in Fig. 4. The numbers mark sources discussed in the text

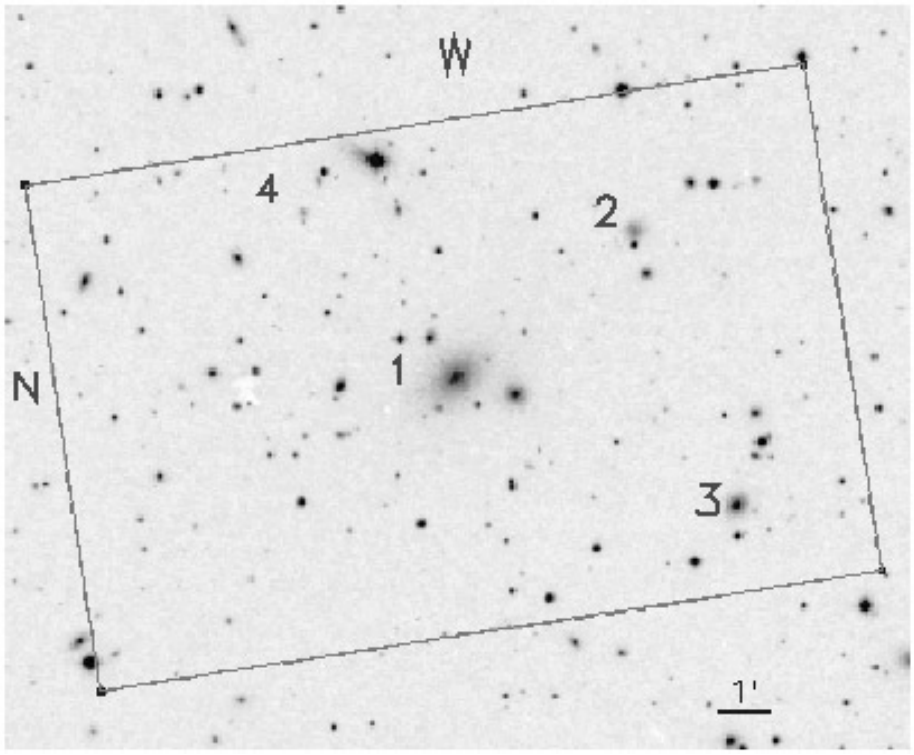


**Fig. 4.** The central field of Abell 2052 showing the boundaries of the C200 map.

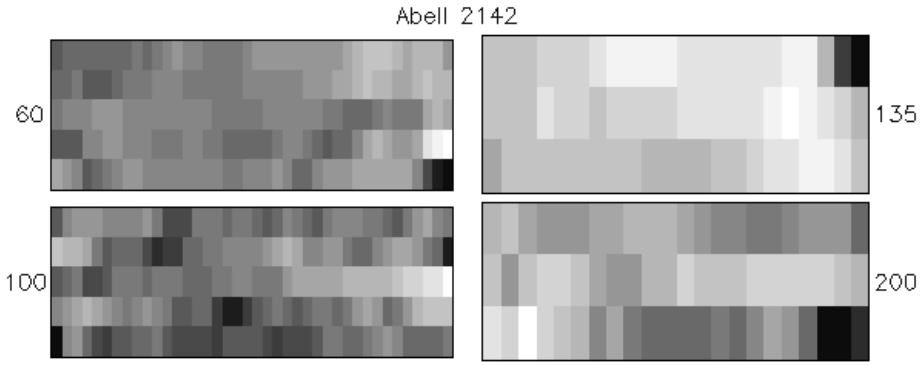


**Fig. 5.** The brightness maps are shown for Abell 2142 for the four pass-bands. Maximum brightness is dark. Value ranges in $\mathrm{MJy\,sr^{-1}}$ are: 6.2–9.7 ($60\,\mu\mathrm{m}$), 5.5–7.9 ($100\,\mu\mathrm{m}$), 7.6–9.8 ($135\,\mu\mathrm{m}$), 5.5–6.5 ($200\,\mu\mathrm{m}$). Left is approximately towards north and up towards west. Compare with the optical image of the field shown in Fig. 6

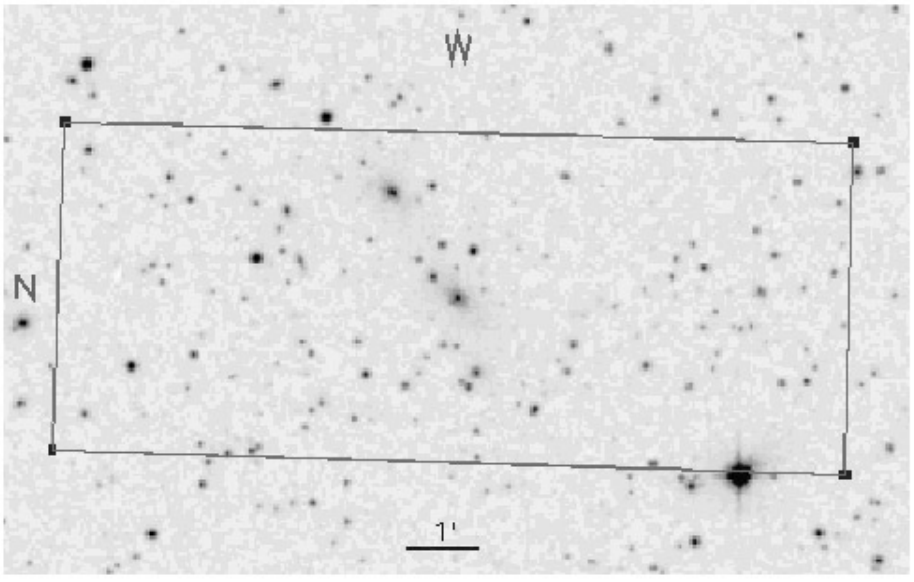


**Fig. 6.** The central field of Abell 2142 showing the boundaries of the C200 map.

**Table 4.** Subjectively estimated upper limits (Jy) on any infrared emission (point source or extended) from the cooling flow are compared with the values derived from a simple model

| | $60\,\mu$m | $100\,\mu$m | $135\,\mu$m | $200\,\mu$m | |
|---|---|---|---|---|---|
| A 2029 | $< 0.09$ | $< 0.07$ | $< 0.18$ | $< 0.22$ | point source |
| | $< 0.38$ | $< 0.23$ | $< 0.21$ | $< 0.31$ | extended |
| | 0.19 | 0.27 | 0.21 | 0.11 | model |
| A 2052 | $< 0.09$ | $< 0.09$ | $< 0.21$ | $< 0.25$ | point source |
| | $< 0.57$ | $< 0.52$ | $< 0.52$ | $< 0.44$ | extended |
| | 0.02 | 0.06 | 0.07 | 0.05 | model |
| A 2142 | $< 0.06$ | $< 0.07$ | $< 0.15$ | $< 0.18$ | point source |
| | $< 0.12$ | $< 0.14$ | $< 0.17$ | $< 0.21$ | extended |
| | 0.22 | 0.18 | 0.11 | 0.05 | model |

by sputtering, and a steady state is obtained. When $\dot{\mathrm{M}}$ and the density and temperature of the hot gas are known from X-ray observations, the model allows us to calculate the total amount of dust present and to predict the far-infrared flux from the heated grains. If these fluxes were actually observed, the formation of stars in cooling flows would be confirmed indirectly.

Hansen et al. (1995) found that the IRAS flux measured from Hydra A was well explained by this model. In paper II we showed that our ISOPHOT data for Sérsic 159-03 were roughly consistent with the model, but we also presented evidence for a recent merger event which could as well be a source of dust. For Abell 2670 the presence of several sources and the limited resolution did not allow us to detect a possible central source of the predicted strength (paper I).

Also for Abell 2029, Abell 2052, and Abell 2142 we find no convincing central source. In an attempt to put limits on a central source which could possibly exclude the model we did as follows: The PSF was multiplied by a factor and added to the center of the maps. By varying the factor we found the minimum detectable flux. We also *subtracted* the scaled PSF until a similar limit was found. The numerical values of the two limits were always similar. The average of the two determinations was accepted as the upper limit for the flux of a possible central point source. The results are given in Table 4. Model calculations similar to those made for Hydra A (Hansen et al. 1995) were performed for Abell 2029, Abell 2052, and Abell 2142 based on the parameters collected in Table 1. These results are also given in Table 4. A comparison between the results shows that the model predictions are sometimes more than 3 times larger than the observed limits. This is, however, not sufficient to exclude the model due to the large uncertainties of the estimates. Furthermore, the source is expected to have a spatial distribution within the cooling radius, $\mathrm{R_{cool}}$. As a "worst case" we repeat the estimate of the limit assuming that the emission is evenly distributed within $\mathrm{R_{cool}}$. This is obtained by convolution of the PSF by a top hat of radius $\mathrm{R_{cool}}$ before adding or subtracting to the brightness maps. As expected the limits are widened, and they now exceed the model predictions in most cases. Thus, we are not able to exclude the model based on the present data.

## 4. Conclusion

Our far-infrared survey of five rich galaxy clusters has shown that even in the limited fields of the survey there are a number of real features. The C200 results are the most reliable because this detector is less sensitive to cosmic ray glitches compared to C100. Unfortunately the spatial resolution of C200 is poor, and it is often uncertain whether we are dealing with filamentary structures or a superposition of unresolved sources. Several sources were, however, identified with cluster galaxies, and some of these show signs of enhanced star formation. In other cases no particular optical counterpart can be attributed. The structured fields have prevented the identification of a firm baseline for flux measurements. Instead we have made subjective estimates by subtraction of a scaled PSF. We typically estimate fluxes for point sources to be $\approx 0.1$ Jy. The complicated fields also hamper the test of our hypothesis of far-infrared emission from the cooling flow, which would indirectly confirm that the cooling gas is transformed into stars. Only for Sérsic 159-03 a flux can be detected which is roughly consistent with the model, but this flux can also be due to an indicated merger event. For the other four objects our observed upper limits are an order of magnitude too high to settle the question.

*Acknowledgements.* This work has been supported by The Danish Board for Astronomical Research.

## References

Hansen L., Jørgensen H.E., Nørgaard-Nielsen H.U., 1995, A&A 297, 13
Hansen L., Jørgensen H.E., Nørgaard-Nielsen H.U., et al., 1999, A&A 349, 406 (paper I)
Hansen L., Jørgensen H.E., Nørgaard-Nielsen H.U., et al., 2000, A&A 356, 83 (paper II)
Henry J.P., Briel U.G., 1996, ApJ 472, 137
Lemke D., Klaas U., Abolins J., et al., 1996, A&A 315, L64
Markevitch M., Ponman T.J., Nulsen P.E.J., et al., 2000, draft paper, astro-ph/0001269
Rizza E., Loken C., Bliton M., et al., 2000, AJ 119, 21
Sarazin C.L., Wise M.W., Markevitch M.L., 1998, ApJ 498, 606
White D.A., Jones C., Forman W., 1997, MNRAS 292, 419